# DESIGN OF PERMANENT MAGNET HYBRID STEPPER MOTOR FOR COGGING TORQUE REDUCTION BY FINITE ELEMENT METHOD USING PDETOOL

**Dr. E.V.C.SEKHARA RAO**
CBIT, Hyderabad, India: 9290448153:drevcsekhararao@cbit.ac.in

***ABSTRACT:*** *This paper is focused on the design of Permanent Magnet Hybrid (PMH) stepper motor magnetic circuit for two Topologies by Finite Element method (FEM) using Partial Differential Equation Tool (PDETOOL) of MATLAB. Two Topologies are; one without extra teeth between main stator poles and the other one is with extra teeth between main stator poles. These two Topologies are analyzed with two different core materials at its half load and full load. Using the results of magnetic potential of these two topologies for above four conditions; a better Topology is concluded which gives rated steady-state torque at rated drive current by reducing cogging torque. A novel experimental method is explained to measure the steady-state torque using PMH stepper motor-generator set.*

***Key words*** *– Cogging torque, FEM, PDETOOL, PMH stepper motor, PMH stepper motor-generator set, Steady-state torque*

## 1. Introduction

This research work is aimed to design a PMH stepper motor to deliver rated steady – state torque at rated drive current. This work is motivated by the design of PMH stepper motor to deliver constant steady-state torque under cryogenic conditions [1]. This work was criticized that the results of [1] are due to the properties of the materials but not due to the design procedure [2]. The design of PMH stepper motor was analyzed using FEM in [2] but concluded that the cogging torque is more and motor was unable to get its steady-state torque at rated drive current.

PMH stepper motor magnetic circuit was analyzed using FEM with different software packages [3] in previous analysis. First time it is analyzed using PDETOOL of Matlab with magnetostatic application. Steady-state and cogging torques have been calculated using Magnetic potential obtained by this analysis.

Tooth layer unit (TLU) concept has been used for analysis [4]. Two Topologies have been designed such that with and without an extra teeth between stator poles. These two Topologies have been analyzed with two different core materials as Iron (99.8%) and Iron (99.95%). This analysis further have been extended for two current levels of half full-load (0.5 A) and full-load (1 A). Steady - state and cogging torques have been calculated [4] for every analysis to obtain the Topology which gives rated steady-state torque at rated current by reducing cogging torque.

Steady – state torque of PMH stepper motor was calculated using sensors in previous analysis [5]. A PMH stepper motor - generator set has been prepared to measure steady – state torque without any sensors to validate the FEM based results obtained by PDETOOL.

## 2. Magnetic Circuit Design

Design of PMH stepper motor magnetic circuit using equivalent circuit model is difficult due to double slotting structure, presence of permanent magnet in the rotor and saturation effects. Hybrid stepper motor has a large number of teeth on the stator and rotor surface and a very small air gap; the magnetic saturation in the teeth becomes severe while increasing the flux density in the airgap. In addition, both radial flux and axial flux are produced because of axially magnetized permanent magnet and geometric characteristics [6]. This makes the analysis of hybrid stepper motor more difficult using two dimensional (2-D) modeling FEM. Three dimensional finite element analyses is one of the solutions for nonlinear analysis of axially unsymmetrical hybrid stepper motor under this situation [7]. But in order to reduce the computational time involved in the analysis, a 2-D equivalent of the three dimensional (3-D) model of

the motor was developed and used. In contrast to other methods, the finite element method accounts for non-homogeneity of the solution region [3]. PMH stepper motor is designed in 2-D for different tooth widths but the design reduces steady state torque and increases cogging torque [2].

Tooth layer unit (TLU) of PMH stepper motor, which is combination of stator and rotor tooth for one tooth pitch, is used for FEM analysis [4, 8]. 2-D Model is used for analysis to get magnetic potential and gap permeance using current density of exciting coil in the stator and permeability of core materials for stator and rotor [9, 10].

## 3. Design Of Topologies Using PDE Toolbox

A practical $1.8^0$ step angle four phase bipolar PMH stepper motor is chosen for design, having 4 poles in the stator and 2 sections in the rotor with 50 teeth on each disk with $AlNiCo_5$ magnet radially magnetized. The main structural parameters of the PMH stepper motor required for Topology design are given in Table 1. Geometry of PMH motor is designed using PDE toolbox GUI for topologies. Airgap length, tooth width and tooth pitch are designed in such a way that ratios of tooth width to tooth pitch is 0.75 and tooth pitch to airgap length is 20. Topologies are designed considering tooth pitch as 1.86 mm, tooth width as 1.42 mm and slot width as 1.32 mm. Two Topologies are designed for analysis, one with conventional stepper motor design and another with an extra tooth between main poles as shown in Fig. 1.

Table 1
Structural Parameters Of Pmh Stepper Motor For Design

| Stator poles | Tooth per stator pole | Outer diameter of stator | Inner diameter of stator | Outer diameter of stator shell |
|---|---|---|---|---|
| 4 | 10 | 10.108 cm | 5.936 cm | 10.652 cm |
| Number of rotor teeth | Number of turns per phase | Section length of rotor | Outer diameter of rotor | Inner diameter of rotor |
| 50 | 102 | 10.26 cm | 4.2 cm | 1.74 cm |

## 4. Magnetic potential Analysis Using FEM

Once geometry for Topologies is designed, boundary conditions are specified for getting vector fields of magnetic potential and flux densities using Magnetostatic application of PDE toolbox. Dirichlet boundary condition is considered as (1, 0) and Neumann boundary condition is considered as (0, 0) for 2-D analysis. Once the boundary conditions are given, programme could be executed to verify correct boundary conditions. After verifying boundary conditions, permeability and current density of different parts like stator core, rotor core, stator current coil and permanent magnet are calculated using eqns. (5), (6) and (7) respectively. Permeability (μ) is one and current density (J) is zero for air-gap.

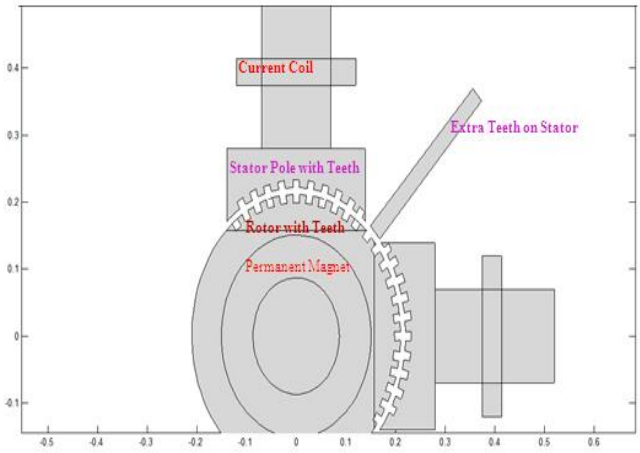


Fig. 1 Geometry design of Topology with an extra teeth between stator poles for a pair of poles

$$\mu = \frac{\mu_{Max}}{1+C\|\nabla^2 A\|} + \mu_{Min} \quad (5)$$

where $\mu_{Max}$, $\mu_{Min}$ are maximum permeability and minimum permeability respectively of core material used for stator and rotor. C is coercive force of the core material. $\nabla^2 A$ is equivalent to $(-\mu J)$ [11].

$$J_c = \frac{\text{Current}}{\text{Area of the conductor}} \quad A/m^2 \ (6)$$

$$J_{pm} = B_s - \mu_0 H_s \quad A/m^2 \quad (7)$$

Two core materials Iron (99.8%) and Iron (99.95%) are considered for analysis. Permeability (μ) is calculated for Iron (99.8%), Iron (99.95%) using eqn.(5) and obtained as 5,150 H/m and 2,10,000 H/m respectively. Standard wire gauge (SWG) 36 conductor is considered for current coil design. Analysis is considered for 0.5A and 1A whose

current densities ($J_c$) are calculated using eqn. (6). Current densities of current coil with 36 SWG conductor for 0.5 A, 1 A are 170648 A/m$^2$ and 341296 A/m$^2$ respectively. Current density ($J_c$) in core materials is equivalent to zero. Current density of permanent Magnet $AlNiCo_5$ is calculated using eqn.7

Fig. 2, shows magnetic potential and flux density vectors diagram with Iron (99.95%) core at current density of 341296 A/m$^2$ (full-load, 1A). Fig. 3 shows at current density of 341296 A/m$^2$ for Iron (99.8%) core for the Topology without extra teeth between main poles

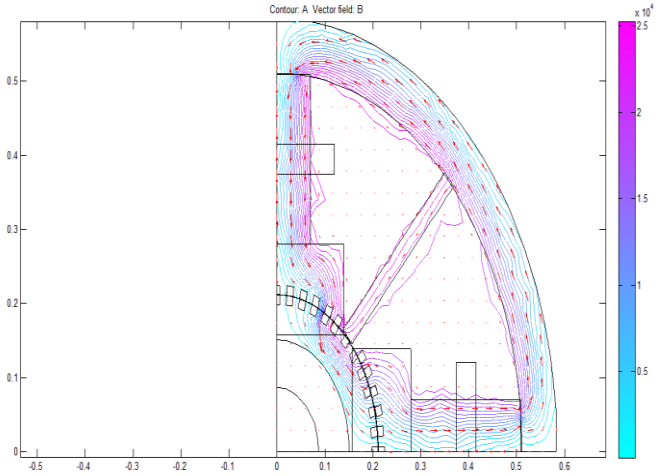


Fig. 2 Magnetic potential and flux density vectors diagram of Topology with extra teeth between main poles with Iron (99.95%) core at current density of 341296 A/m$^2$

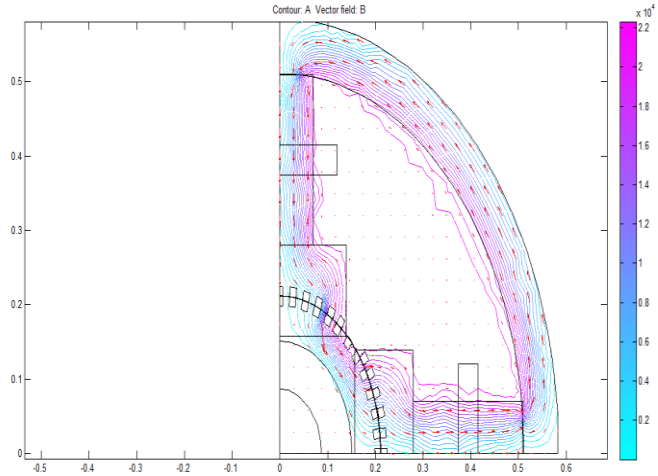


Fig. 3 Magnetic potential and flux density vectors diagram of Topology without an extra teeth between main poles with Iron (99.95%) core at current density of 341296 A/m$^2$

Designed Topologies are executed for mesh generation, when boundary conditions are properly mentioned and PDE coefficients (permeability and current density) for all parts of the Topology are mentioned. Solution for magnetic potential and flux density vectors for the Topologies are obtained through nonlinear solution.

It is observed from this analysis that leakage flux is minimized using extra teeth between main stator poles

## 5. Steady State Torque And Cogging Torque

Steady-state torque and cogging torque of PMH stepper motor are derived in terms of air-gap permeance for one pole pitch. A magnetic equivalent circuit of a 4 pole PMH stepper motor is shown in Fig. 4 whose geometric design parameters are given in Table 1. The subscripts 1,2,3,4 and M denote the poles 1,2,3,4 and the permanent magnet respectively. φ is flux through the respective poles and the permanent magnet, F represents magneto motive forces (MMF) supplied by winding currents and the permanent magnet. $F_0$ is the MMF drop across the air gap, and P represents respective air gap permeance. For the PMH stepper motor, windings 1 and 3 are connected in series, hence F1= - $F_3$. The same is true for windings 2 and 4, so $F_2$ = - $F_4$.

The gap permeance is the fundamental factor affecting torque, inductance and speed of the motor [12, 13]. It relates tooth dimensions of the motor to other parameters, and a design goal is to select tooth geometry in such a way that an optimum motor performance can be realized. Flux lines emanate from the upper teeth and enter the lower ones. The flux flowing directly downward gives radial force on the rotor, which is an order of magnitude greater than the useful force and it is a good design practice to balance this radial force by having an identical pole on the opposite side of the rotor. Otherwise, a strong force will be exerted on the bearings, resulting in greater bearing friction and shorter bearing life. Since the rotor and stator teeth are in relevant motion. The gap permeances ($P_1$ to $P_5$) are calculated using eqn. (8) [13].

$$\begin{bmatrix} P_1 = \mu_0 \frac{t-x}{g} \\ P_2 = \mu_0 \frac{2}{\Pi} \ln\left(1 + \frac{\Pi x}{2g}\right) \\ P_3 = \mu_0 \frac{1}{\Pi} \ln\left(\frac{g+2d-\frac{1}{2}\Pi x}{g+\frac{1}{2}\Pi x}\right) \\ P_4 = \mu_0 \frac{2}{\Pi} \ln\left(\frac{g+2d}{g+2d+\frac{1}{2}\Pi x}\right) \\ P_5 = \mu_0 \frac{T_P - x - \frac{4d}{\Pi}}{g+2d} \end{bmatrix} \quad (8)$$

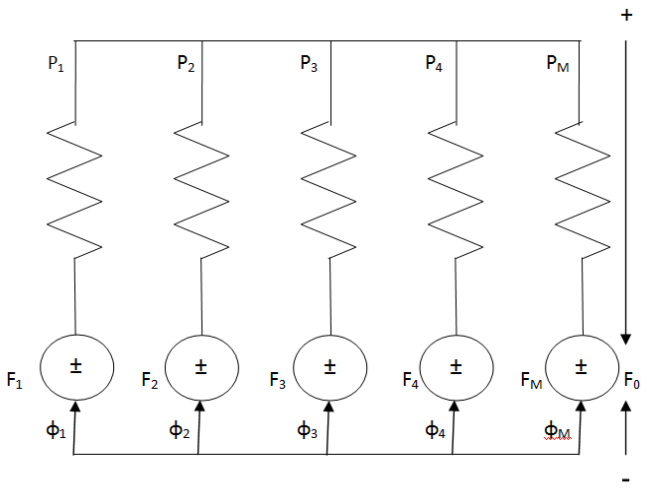


Fig. 4 Magnetic equivalent circuit of 4 pole PMH stepper motor

In eqn. (8) 'x' is considered as equivalent length of step angle ($1.8^0$) and calculated as

$$x = (\frac{1.8}{360} \times \text{circumference of rotor outer circle})$$
$$= 0.659 \text{ mm}$$

For the analysis, tooth width, t = 1.32 mm, tooth pitch, $T_P$ = 1.42 mm, tooth depth, d = 1.32 mm, airgap length, g = 0.137 mm and 0.93 mm are considered. Number of teeth per stator pole, $Z_s$ = 10 when extra teeth between stator poles are not considered and $Z_s$ = 11 when extra teeth between stator poles are considered. The total permeance per pole, $P_t$ is calculated using eqn. (9), considering $P_1$ to $P_5$ are in parallel.

$$P_t = Z_s [P_l + 2(P_2 + P_3 + P_4) + P_5] \text{ H/m} \quad (9)$$

The airgap Permeance per pole is periodic with respect to electric step angle $\theta_e$ and it is expressed in Fourier series when single phase is energized as shown in eqn. (10)

$$P = \rho_0 + \sum_{n=1}^{\infty} \rho_n \cos(n\theta_e), \quad \text{where } n=1, 2, 3\ldots \quad (10)$$

Since the displacement is from $\theta_e$ = 0 to 2π radians corresponds to one-pitch of a tooth, $\rho_0$ is DC component of Fourier coefficient for gap permeance, $\rho_n$ is $n^{th}$ component of Fourier coefficient for gap permeance. The electric step angle, $\theta_e$ is related to the mechanical step angle, $\theta_m$ as shown in eqn. (11), where $Z_R$ is the number of teeth of the rotor.

$$\theta_e = Z_R \theta_m \quad (11)$$

For a four phase motor under analysis, when single phase is energized MMF (F) of different phases is shown in eqn. (12) and Steady-state torque $T_s$ is shown in eqn. (13) [13, 14 and 15]

$$F_1 = -F3 = -NI \text{ and } F_2 = -F_4 = 0 \quad (12)$$

$$T_s = -K.I\left(\sin\theta_e - \frac{NI\rho_1}{F_M P_M}\sin 2\theta_e\right) + \nabla T \text{ Nm} \quad (13)$$

where I is exciting coil current in Amperes and ∇T shows higher order torque terms and the torque constant K is shown in eqn. (14)

$$K = 2N Z_R (F_M P_M)\frac{\rho_1}{\rho_0} \text{ Nm/A} \quad (14)$$

where $F_M$ is MMF of permanent magnet and $P_M$ is permeance of permanent magnet K is proportional to permanent magnet flux ($P_M F_M$), $\frac{\rho_1}{\rho_0}$, number of total rotor teeth per disk, $Z_R$ and number of exciting coil turns N. Permanent magnet flux is obtained from demagnetizing curve of permanent magnet, which is very difficult to evaluate using permeance model. Results using FEM are used to calculate steady-state torque for different topologies. Higher order torque terms are omitted for steady-state torque. Substituting eqn. (14) in eqn. (13) and neglecting ∇T, steady-state torque ($T_s$) is shown in eqn. (15)

$$T_s = -2(NI)Z_R (F_M P_M)\frac{\rho_1}{\rho_0}\left(\sin\theta_e - \frac{NI\rho_1}{F_M P_M}\sin 2\theta_e\right) \quad (15)$$

In general, $NI\rho_1 << (F_M P_M)$. Therefore second term in eqn (4.7) is negligible and the steady-state torque is now shown in eqn. (16)

$$T_s = -2(NI)Z_R (F_M P_M)\frac{\rho_1}{\rho_0}\sin\theta_e \quad (16)$$

Cogging or detent torque exists due to permanent magnet flux even under the absence of excitation, i.e., $F_i$ = 0, where i = 1, 2, 3, 4. For a 4 pole machine, this torque is due to the $4^{th}$ harmonic component of the gap permeance and has a four cycle variation for one tooth pitch. Other multiples of the $4^{th}$ harmonic component of the gap permeance exist, but their magnitudes are negligible. With this concept, cogging torque is shown in eqn. (17) [16, 17]

$$T_{cog} = \frac{Z_R}{2}\left(\frac{F_M P_M}{\rho_0}\right)^2 \rho_4 \sin 4\theta_e \quad (17)$$

Fig. 5 shows steady state torque 3-D plot of Topology with extra teeth between main poles for Iron (99.95%) core to both step angle and full load exciting current (1A). Fig. 6 shows steady state torque 3-D plot of Topology

without extra teeth between main poles for Iron (99.95%) core to both step angle and full load exciting current (1A).

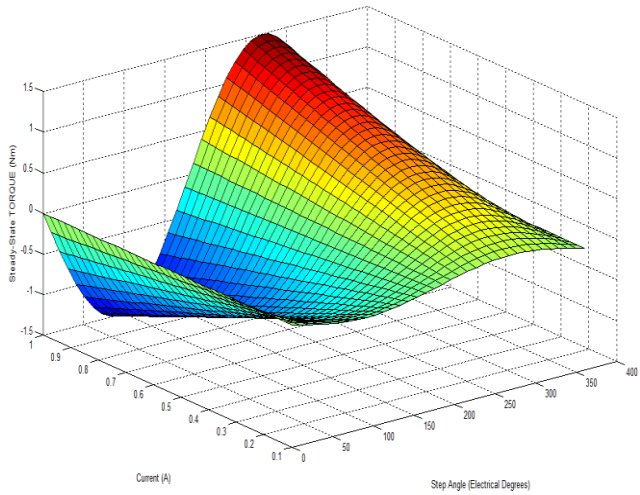


Fig. 5 Steady-state torque 3-D plot of Topology with extra teeth between main poles for Iron (99.95%) core to both step angle and exciting current

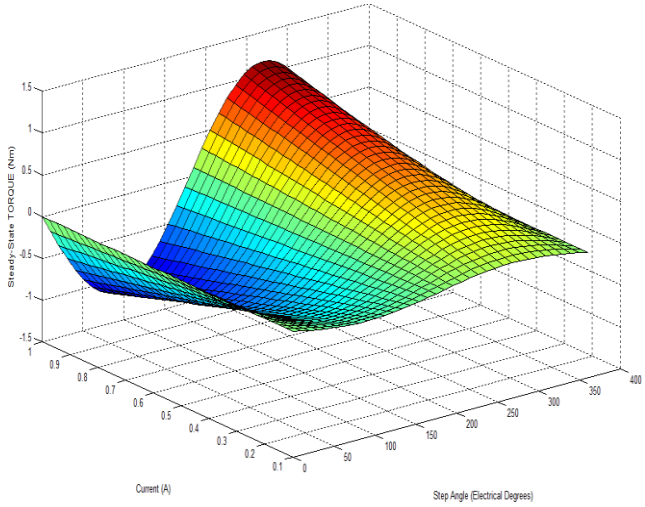


Fig. 6 Steady-state torque 3-D plot of Topology without extra teeth between main poles for Iron (99.95%) core to both step angle and exciting current

Fig. 7 shows steady-state torques & cogging torques of Topology with extra teeth between main poles for Iron (99.8%) & Iron (99.95%) cores at exciting currents of 0.5 A & 1 A. Fig. 8 shows steady-state torques & cogging torques of Topology without extra teeth between main poles for Iron (99.8%) & Iron (99.95%) cores at exciting currents of 0.5 A & 1 A.

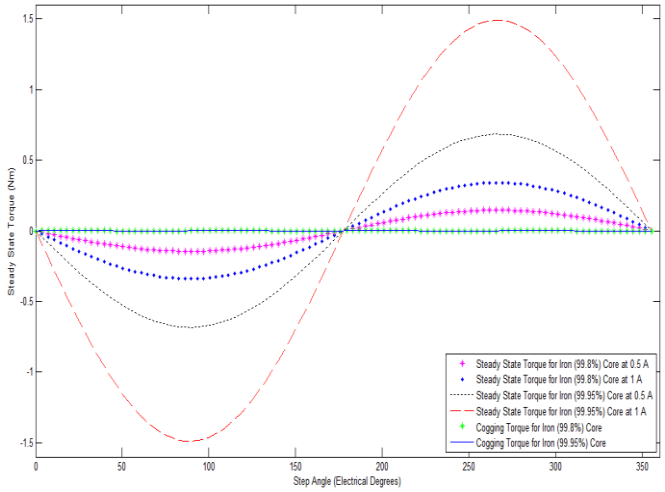


Fig. 7 Steady-state torques & cogging torques of Topology with extra teeth between main poles for Iron (99.8%), Iron (99.95%) cores at an exciting currents of 0.5 A & 1 A

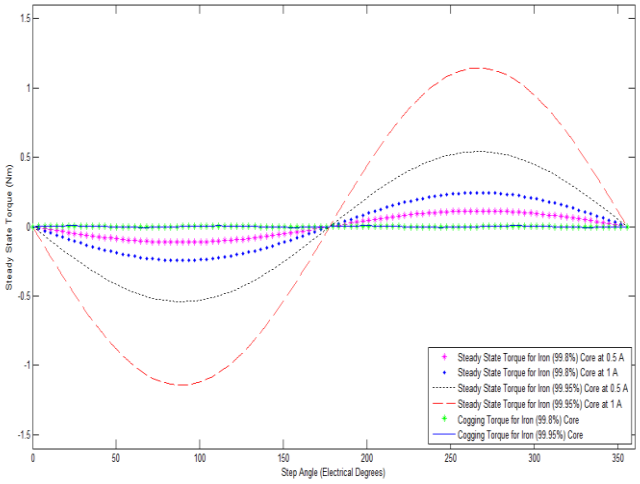


Fig. 8 Steady-state torques & cogging torques of Topology with extra teeth between main poles for Iron (99.8%), Iron (99.95%) cores at an exciting currents of 0.5 A & 1 A

Topology with extra teeth between stator poles design with Iron (99.95%) at rated excitation current (1 A) is able to produce rated steady state torque (1.4907 Nm of 1.5 Nm) with low cogging torque (0.0051 Nm) and with maximum steady state torque to cogging torque ratio (270.9) when compared to the Topology without extra teeth between stator poles whose steady state torque is unable to reach rated value at rated current (1.14 Nm of 1.5 Nm) with more cogging torque (0.0061 Nm) and with minimum steady state torque to cogging torque ratio (187.25).

## 6. Experimental Validation Of The Designed Topology

A novel experimental set-up is arranged to measure steady state torque of Topology without extra teeth between stator poles not using any sensors. A prototype motor which is considered for experiment is having the design specifications as shown in TABLE 1. Two such identical PMH stepper motors of same rating of 1.5 Nm are coupled using special aluminum coupling forming PMH stepper motor-generator set as shown in Fig. 9. This arrangement forms PMH stepper motor-generator set. One of the machines in this set is excited programmatically through DSP processor working as PMH stepper motor and drives the other machine which works as generator and induces voltage in the phase windings. The speed of the motor is increased by increasing drive speed in steps/second by varying time constant in the DSP processor programme which controls PMH stepper motor excitation sequence. This generated voltage in the generator mode machine phase windings is measured at no-load and speed is measured at different load currents by applying resistive load. The Proto type PMH stepper motor - generator diagram of experimental setup is shown in Fig. 10.

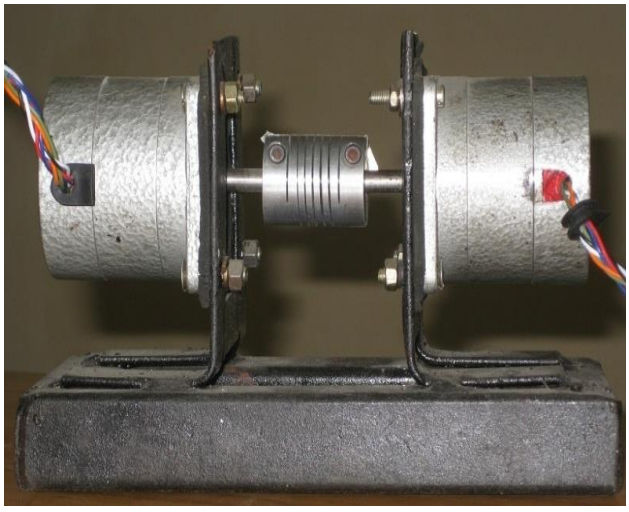

Fig. 9 Prototype PMH stepper motor-generator set

The speed of the motor is varied from 1 rad. / sec to 30 rad. / sec by varying time constant in DSP IC and corresponding generated voltages are measured and tabled in Table 2. Fig. 10 shows relation between PMH stepper generator generated voltage in Volts to speed in radians/second. A resistive load (0 – 25Ω) is connected to generator mode machine terminals. Speed of the motor is noted down at different load currents of generator and shown in Table 3. The relation between speed in rad. / sec and load current in A is shown in Fig. 11.

From the results of no-load and load tests on PMH stepper motor-generator set, steady-state torque is calculated and is shown in Table 4.

Table 2 No-load induced voltages in PMH stepper generator at different speeds

| Speed (radians/second) | 0 | 05 | 10 | 20 | 30 |
|---|---|---|---|---|---|
| No-load induced voltage (V) | 0 | 5.8 | 11.6 | 23 | 34 |

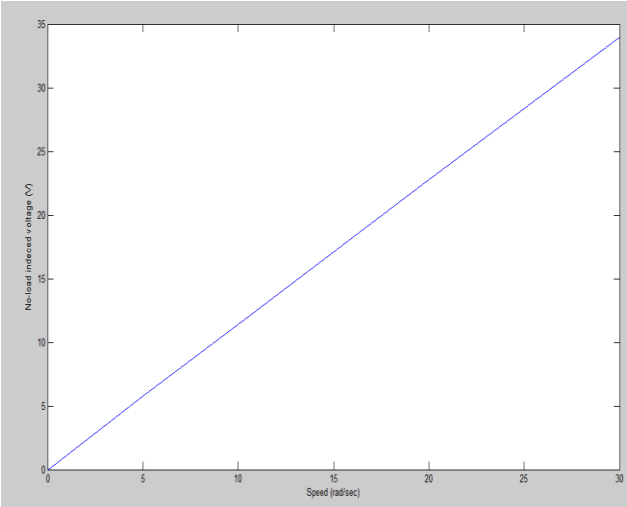


Fig.10 No-load Induced voltages in PMH generator at different Speeds

Table 3 PMH motor Speeds and no-load induced voltages at different load currents

| Load current (A) | 0.2 | 0.5 | 1 | 1.5 |
|---|---|---|---|---|
| Speed (rad. /sec) | 30 | 29 | 28 | 27 |
| No-load induced voltage (V) | 34 | 32.5 | 30.8 | 27.2 |

Table 4 Steady-state torque of PMH stepper motor at different load currents with the corresponding speeds

| Current (A) | 0.2 | 0.5 | 1 | 1.5 |
|---|---|---|---|---|
| Speed (radians/second) | 30 | 29 | 28 | 27 |
| steady-state torque (Nm) | 0.23 | 0.56 | 1.1 | 1.51 |

Speed corresponding to rated current 1 A is obtained as 28 radians/second from load characteristic. No-load induced voltage corresponding to this speed of the motor is obtained as 28.5 V from no-load characteristic. The product of no-load voltage and load current of PMH generator is considered as input of generator mode

machine which is equal to mechanical output of PMH stepper motor. Torque of PMH stepper motor is obtained dividing this power with corresponding angular speed. The corresponding toque calculated at rated current of the motor (1 A) is equal to 1.1 Nm. The same procedure is repeated at 1.5 A load current and torque calculated is equal to 1.51 Nm.

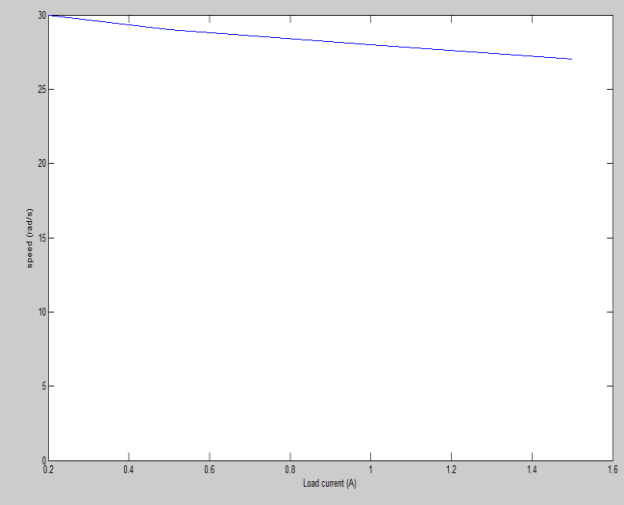

Fig. 11 PMH motor speed at different load currents

Fig. 10 Proto type PMH stepper motor - generator experimental setup

## 7. Conclusions

Finally it is concluded that when an extra teeth is not provided between stator poles of PMH stepper motor its steady-state torque is not obtained at rated drive current as its cogging torque is more. When an extra tooth is provided between stator poles, its steady-state torque is obtained at rated drive current for Iron (99.95%) core material as its cogging torque is reduced.

References

[1] K. R. Rajagopal, M. Krishnaswammy, Bhim Singh and B. P. Singh, 'An Improved High- Resolution Hybrid Stepper Motor for Solar-Array Drive of Indian Remote- Sensing Satellite', IEEE Transactions on Industry Applications, Vol.33, No. 4, July/August 1997

[2] Praveen R.P, Ravichandran M.H, V.T. Sadasivan Achari, Dr.Jagathy Raj V. P, Dr.G.Madhu and Dr.G.R. Bindu, 'Design and Finite Element Analysis of Hybrid Stepper Motor for Spacecraft Applications', IEEE Transactions on Magnetics, Vol.45, No. 4, July/August. 2009

[3] i-Chae Lim, Jung-Pyo Hong, 'Characteristic Analysis of 5-phase Hybrid Stepping Motor Considering the Saturation Effect', IEEE Transactions on Industry Applications, Vol.37, No. 4, July/August 2001, pp. 289–294

[4] Dou Yiping, 'The Engineering Rationality of a Hybrid Stepping Motor Calculation Model', Proceedings of the CSEE, vol. 19, no. 5, pp. 35-38, May. 1999

[5] Ja.Alvarez-Gallegos, E. Alvarez-Sanchez and R. Castro-Linares 'Experimental Setup for the Sensor less Rotor Position Control of a Permanent Magnet Stepper Motor', Proc. IEEE/IAS Annual Meeting, 2004

[6] M. K. Jenkins, D. Howe and T. S. Brich, 'An improved design procedure for hybrid stepper motor', IEEE Transaction on magnetic, Vol.26, pp.2535-2537, 2009

[7] Ki-Bong Jang, Seong-Y eop Lim, Tae-Bin Lim and Ju Lee, '2-D FEM Analysis of Hybrid Stepping Motor using Virtual Magnetic Barrier', IEEE Transaction on magnetic, Vol.39, No 5, pp.3268-3270, 2003

[8] Ibrahim Mahariq, "A Normalized Set of Force and Permeance Data for Doubly Salient Magnetic Geometries", PhD Thesis, Middle East Technical University, department of Electrical and Electronic Engineering, 2009

[9] Jiaxin Chen, Jianguo Zhu, Youguang Guo, 'A 2-D Nonlinear FEA Tool Embedded in Matlab/Simulink Surrounding for Application of Electromagnetic Field Analysis in Power Converters', Proceeding of International Conference on Electrical Machines and Systems 2007, Oct. 8~11, Seoul, Korea

[10] Albanese, R. and Rubinacci, G, 'Numerical

Procedures for the Solution of Nonlinear Electromagnetic Problems', IEEE Transactions on Magnetics, Vol. 28, No. 2, March 1992, pp.1228–1231

[11] Karl J. Strnat, 'Modern Permanent Magnets for Applications in Electro-Technology', Proceedings of the IEEE, Volume 78, Number 6, June 1990

[12] K. C. Mukkarji, 'Magnetic Permeance of Identical Double Slotting Deduction from Analysis by F. W. Carter', IEE, volume 118, No.9, September 1971

[13] Cornelia Stuebig, Bernd Ponick, 'Determination of Air Gap Permeances of Hybrid Stepping Motors for Calculation of Motor Behavior', IEEE International Conference on Electrical Machines, 978-1-4244-1736-0/08, 2008

[14] Kuo.B.C, Chen.Y.I, 'A nonlinear magnetic circuit model and its application to holding torque production of hybrid stepper motor', 13th IMCSD Symposium, pp.303-313, 1984

[15] V.V. Athani, "Stepper motors fundamentals, applications and design", New Age International Limited, India. 1997

[16] D. Lin, P. Zhou and Z. J. Cendes, 'Analytical Prediction of Cogging Torque in Spoke Type Permanent Magnet Motors', IEEE International Conference on Electrical machines, 978-1-4244-1736-0/08, 2008

[17] Fengge Zhang, Ningze Tong, Fengxiang Wang, 'Study on Cogging Torque Reduction Methods of PM Stepping Motor', IEEE International Conference on Power System Technology, POWERCON 2004, Singapore, 21-24 November 2004